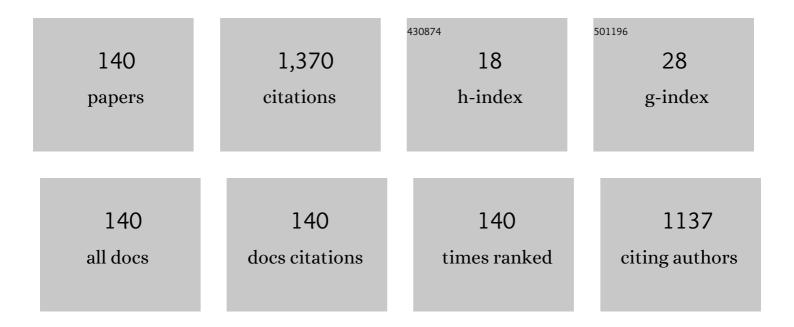
List of Publications by Year in descending order

Source: https://exaly.com/author-pdf/9358435/publications.pdf Version: 2024-02-01



HONG-XIA LILL

#	Article	lF	CITATIONS
1	Symmetric U-Shaped Gate Tunnel Field-Effect Transistor. IEEE Transactions on Electron Devices, 2017, 64, 1343-1349.	3.0	81
2	Design of High Performance Si/SiGe Heterojunction Tunneling FETs with a T-Shaped Gate. Nanoscale Research Letters, 2017, 12, 198.	5.7	56
3	Analog/RF Performance of T-Shape Gate Dual-Source Tunnel Field-Effect Transistor. Nanoscale Research Letters, 2018, 13, 321.	5.7	53
4	TCAD Simulation of Single-Event-Transient Effects in L-Shaped Channel Tunneling Field-Effect Transistors. IEEE Transactions on Nuclear Science, 2018, 65, 2250-2259.	2.0	42
5	Tunable graphene-based hybrid plasmonic modulators for subwavelength confinement. Scientific Reports, 2017, 7, 5190.	3.3	40
6	Physical properties and electrical characteristics of H2O-based and O3-based HfO2 films deposited by ALD. Microelectronics Reliability, 2012, 52, 1043-1049.	1.7	38
7	A Multi-level Memristor Based on Al-Doped HfO2 Thin Film. Nanoscale Research Letters, 2019, 14, 177.	5.7	38
8	Reduced Miller Capacitance in U-Shaped Channel Tunneling FET by Introducing Heterogeneous Gate Dielectric. IEEE Electron Device Letters, 2017, 38, 403-406.	3.9	33
9	Self-Compliance and High Performance Pt/HfOx/Ti RRAM Achieved through Annealing. Nanomaterials, 2020, 10, 457.	4.1	28
10	Probing the Optical Properties of MoS2 on SiO2/Si and Sapphire Substrates. Nanomaterials, 2019, 9, 740.	4.1	25
11	Simulation and Performance Analysis of Dielectric Modulated Dual Source Trench Gate TFET Biosensor. Nanoscale Research Letters, 2021, 16, 34.	5.7	25
12	A Novel Dopingless Fin-Shaped SiGe Channel TFET with Improved Performance. Nanoscale Research Letters, 2020, 15, 202.	5.7	25
13	Analog/RF performance of L- and U-shaped channel tunneling field-effect transistors and their application as digital inverters. Japanese Journal of Applied Physics, 2017, 56, 064102.	1.5	23
14	Defect Detection of IC Wafer Based on Spectral Subtraction. IEEE Transactions on Semiconductor Manufacturing, 2010, 23, 141-147.	1.7	22
15	Optical Transport Properties of Graphene Surface Plasmon Polaritons in Mid-Infrared Band. Crystals, 2019, 9, 354.	2.2	22
16	Volatile and Nonvolatile Memory Operations Implemented in a Pt/HfOâ,,/Ti Memristor. IEEE Transactions on Electron Devices, 2021, 68, 1622-1626.	3.0	22
17	Hybrid Tube-Triangle Plasmonic Waveguide for Ultradeep Subwavelength Confinement. Journal of Lightwave Technology, 2017, 35, 2259-2265.	4.6	21
18	Magnetism investigation of GaN monolayer doped with group VIII B transition metals. Journal of Materials Science, 2018, 53, 15986-15994.	3.7	20

#	Article	IF	CITATIONS
19	Structural Properties Characterized by the Film Thickness and Annealing Temperature for La2O3 Films Grown by Atomic Layer Deposition. Nanoscale Research Letters, 2017, 12, 233.	5.7	19
20	Multi-Level Switching of Al-Doped HfO2 RRAM with a Single Voltage Amplitude Set Pulse. Electronics (Switzerland), 2021, 10, 731.	3.1	19
21	Improvement of Electrical Performance in Heterostructure Junctionless TFET Based on Dual Material Gate. Applied Sciences (Switzerland), 2020, 10, 126.	2.5	18
22	Defect detection of IC wafer based on two-dimension wavelet transform. Microelectronics Journal, 2010, 41, 171-177.	2.0	17
23	The influence of process parameters and pulse ratio of precursors on the characteristics of La1 â^' x Al x O3 films deposited by atomic layer deposition. Nanoscale Research Letters, 2015, 10, 180.	5.7	17
24	Theoretical research of diluted magnetic semiconductors: GaN monolayer doped with transition metal atoms. Superlattices and Microstructures, 2018, 120, 382-388.	3.1	16
25	Sensitivity Analysis of Biosensors Based on a Dielectric-Modulated L-Shaped Gate Field-Effect Transistor. Micromachines, 2021, 12, 19.	2.9	16
26	Silicon diffusion control in atomic-layer-deposited Al2O3/La2O3/Al2O3 gate stacks using an Al2O3 barrier layer. Nanoscale Research Letters, 2015, 10, 141.	5.7	15
27	Impacts of Cu-Doping on the Performance of La-Based RRAM Devices. Nanoscale Research Letters, 2019, 14, 224.	5.7	15
28	Analog/RF performance of four different Tunneling FETs with the recessed channels. Superlattices and Microstructures, 2016, 100, 1238-1248.	3.1	14
29	Modulation speed limits of a graphene-based modulator. Optical and Quantum Electronics, 2018, 50, 1.	3.3	14
30	Design and Investigation of the Junction-Less TFET with Ge/Si0.3Ge0.7/Si Heterojunction and Heterogeneous Gate Dielectric. Electronics (Switzerland), 2019, 8, 476.	3.1	14
31	Negative differential resistance in single-walled SiC nanotubes. Science Bulletin, 2008, 53, 3770-3772.	1.7	13
32	Monte Carlo calculation of electron diffusion coefficient in wurtzite indium nitride. Applied Physics Letters, 2012, 100, 142105.	3.3	13
33	Electrical performance of InAs/GaAs _{0.1} Sb _{0.9} heterostructure junctionless TFET with dual-material gate and Gaussian-doped source. Semiconductor Science and Technology, 2020, 35, 095004.	2.0	13
34	Two ESD Detection Circuits for 3\$imes\$ VDD-Tolerant I/O Buffer in Low-Voltage CMOS Processes With Low Leakage Currents. IEEE Transactions on Device and Materials Reliability, 2013, 13, 319-321.	2.0	12
35	Design and investigation of a dual source and U-shaped gate TFET with n buffer and SiGe pocket. AIP Advances, 2020, 10, .	1.3	12
36	An analytical model of low field and high field electron mobility in wurtzite indium nitride. Journal of Materials Science: Materials in Electronics, 2016, 27, 11353-11357.	2.2	11

#	Article	IF	CITATIONS
37	A 130 GHz Electro-Optic Ring Modulator with Double-Layer Graphene. Crystals, 2017, 7, 65.	2.2	11
38	Graphene-Hexagonal Boron Nitride Heterostructure as a Tunable Phonon–Plasmon Coupling System. Crystals, 2017, 7, 49.	2.2	11
39	Electrical Properties and Interfacial Issues of HfO2/Ge MIS Capacitors Characterized by the Thickness of La2O3 Interlayer. Nanomaterials, 2019, 9, 697.	4.1	11
40	Fabrication and Characterization of MoS2/h-BN and WS2/h-BN Heterostructures. Micromachines, 2020, 11, 1114.	2.9	11
41	TCAD simulation of a double Lâ€shaped gate tunnel fieldâ€effect transistor with a covered source–channel. Micro and Nano Letters, 2020, 15, 272-276.	1.3	11
42	Identification of optimal ALD process conditions of Nd2O3 on Si by spectroscopic ellipsometry. Applied Physics A: Materials Science and Processing, 2014, 114, 545-550.	2.3	10
43	A high performance Ge/Si 0.5 Ge 0.5 /Si heterojunction dual sources tunneling transistor with a U-shaped channel. Superlattices and Microstructures, 2017, 106, 8-19.	3.1	10
44	Probing the Field-Effect Transistor with Monolayer MoS2 Prepared by APCVD. Nanomaterials, 2019, 9, 1209.	4.1	10
45	A Horizontal-Gate Monolayer MoS2 Transistor Based on Image Force Barrier Reduction. Nanomaterials, 2019, 9, 1245.	4.1	10
46	Design and Investigation of the High Performance Doping-Less TFET with Ge/Si0.6Ge0.4/Si Heterojunction. Micromachines, 2019, 10, 424.	2.9	10
47	Design and investigation of dopingless dual-gate tunneling transistor based on line tunneling. AIP Advances, 2019, 9, .	1.3	10
48	A New Electro-Optical Switch Modulator Based on the Surface Plasmon Polaritons of Graphene in Mid-Infrared Band. Sensors, 2019, 19, 89.	3.8	10
49	Performance investigations of novel dual-material gate (DMG) MOSFET with dielectric pockets (DP). Science in China Series D: Earth Sciences, 2009, 52, 2400-2405.	0.9	9
50	Influence of different oxidants on the band alignment of HfO 2 films deposited by atomic layer deposition. Chinese Physics B, 2012, 21, 087702.	1.4	9
51	A novel Ge based overlapping gate dopingless tunnel FET with high performance. Japanese Journal of Applied Physics, 2019, 58, 100902.	1.5	9
52	A Doping-Less Tunnel Field-Effect Transistor with Si0.6Ge0.4 Heterojunction for the Improvement of the On–Off Current Ratio and Analog/RF Performance. Electronics (Switzerland), 2019, 8, 574.	3.1	9
53	Probing the Growth Improvement of Large-Size High Quality Monolayer MoS2 by APCVD. Nanomaterials, 2019, 9, 433.	4.1	9
54	First-Principles Study on the Effect of Strain on Single-Layer Molybdenum Disulfide. Nanomaterials, 2021, 11, 3127.	4.1	9

#	Article	IF	CITATIONS
55	Optical characteristics of H2O-based and O3-based HfO2 films deposited by ALD using spectroscopy ellipsometry. Applied Physics A: Materials Science and Processing, 2015, 119, 957-963.	2.3	8
56	Impacts of Annealing Conditions on the Flat Band Voltage of Alternate La2O3/Al2O3 Multilayer Stack Structures. Nanoscale Research Letters, 2016, 11, 394.	5.7	8
57	Design and Investigation of a Dual Material Gate Arsenic Alloy Heterostructure Junctionless TFET with a Lightly Doped Source. Applied Sciences (Switzerland), 2019, 9, 4104.	2.5	8
58	Graphene Electro-Optical Switch Modulator by Adjusting Propagation Length Based on Hybrid Plasmonic Waveguide in Infrared Band. Sensors, 2020, 20, 2864.	3.8	8
59	Electrical Phase Control Based on Graphene Surface Plasmon Polaritons in Mid-infrared. Nanomaterials, 2020, 10, 576.	4.1	8
60	Research on the Preparation and Spectral Characteristics of Graphene/TMDs Hetero-structures. Nanoscale Research Letters, 2020, 15, 219.	5.7	8
61	Modeling and Simulation of Hafnium Oxide RRAM Based on Oxygen Vacancy Conduction. Crystals, 2021, 11, 1462.	2.2	8
62	Influences of different oxidants on the characteristics of HfAlO _{<i>x</i>} films deposited by atomic layer deposition. Chinese Physics B, 2013, 22, 027702.	1.4	7
63	The optical properties of GaN (001)surface modified by intrinsic defects from density functional theory calculation. Optik, 2018, 154, 378-382.	2.9	7
64	A Long Propagation Distance Hybrid Triangular Prism Waveguide for Ultradeep Subwavelength Confinement. IEEE Sensors Journal, 2019, 19, 11159-11166.	4.7	7
65	Improved resistive switching characteristics of atomic layer deposited Al2O3/La2O3/Al2O3 multi-stacked films with Al+ implantation. Journal of Materials Science: Materials in Electronics, 2019, 30, 12577-12583.	2.2	7
66	Wide-Range Tunable Narrow Band-Stop Filter Based on Bilayer Graphene in the Mid-Infrared Region. IEEE Photonics Journal, 2020, 12, 1-9.	2.0	7
67	The Large-Scale Preparation and Optical Properties of MoS2/WS2 Vertical Hetero-Junction. Molecules, 2020, 25, 1857.	3.8	7
68	Frequency dispersion effect and parameters extraction method for novel HfO2 as gate dielectric. Science China Information Sciences, 2010, 53, 878-884.	4.3	6
69	Influences of rapid thermal annealing on the characteristics of Al2O3La2O3Si and La2O3Al2O3Si films deposited by atomic layer deposition. Journal of Materials Science: Materials in Electronics, 2016, 27, 8550-8558.	2.2	6
70	The Study of Electrical Properties for Multilayer La2O3/Al2O3 Dielectric Stacks and LaAlO3 Dielectric Film Deposited by ALD. Nanoscale Research Letters, 2017, 12, 230.	5.7	6
71	Effects of Annealing Ambient on the Characteristics of LaAlO3 Films Grown by Atomic Layer Deposition. Nanoscale Research Letters, 2017, 12, 108.	5.7	6
72	Research on the Factors Affecting the Growth of Large-Size Monolayer MoS2 by APCVD. Materials, 2018, 11, 2562.	2.9	6

#	Article	IF	CITATIONS
73	Study of a Gate-Engineered Vertical TFET with GaSb/GaAs0.5Sb0.5 Heterojunction. Materials, 2021, 14, 1426.	2.9	6
74	Impacts of LaOx Doping on the Performance of ITO/Al2O3/ITO Transparent RRAM Devices. Electronics (Switzerland), 2021, 10, 272.	3.1	6
75	A high performance trench gate tunneling field effect transistor based on quasi-broken gap energy band alignment heterojunction. Nanotechnology, 2022, 33, 225205.	2.6	6
76	Monte Carlo transport simulation of velocity undershoot in zinc blende and wurtzite InN. Physica Status Solidi (B): Basic Research, 2012, 249, 1761-1764.	1.5	5
77	Improvement of the Anneal-Induced Valence Band Offset Variation by the Hybrid Deposition of \${m HfO}_{2}\$ on Si. IEEE Transactions on Electron Devices, 2013, 60, 1536-1539.	3.0	5
78	Band alignments of O3-based and H2O-based amorphous LaAlO3 films on silicon by atomic layer deposition. Journal of Materials Science: Materials in Electronics, 2017, 28, 803-807.	2.2	5
79	The Programming Optimization of Capacitorless 1T DRAM Based on the Dual-Gate TFET. Nanoscale Research Letters, 2017, 12, 524.	5.7	5
80	Electron Momentum and Energy Relaxation Times in Wurtzite GaN, InN and AlN: A Monte Carlo Study. Journal of Electronic Materials, 2018, 47, 1560-1568.	2.2	5
81	Improvements on the Interfacial Properties of High-k/Ge MIS Structures by Inserting a La2O3 Passivation Layer. Materials, 2018, 11, 2333.	2.9	5
82	Effect of the High-Temperature Off-State Stresses on the Degradation of AlGaN/GaN HEMTs. Electronics (Switzerland), 2019, 8, 1339.	3.1	5
83	Study on Single Event Effect Simulation in T-Shaped Gate Tunneling Field-Effect Transistors. Micromachines, 2021, 12, 609.	2.9	5
84	Investigation of charge trapping mechanism in MoS ₂ field effect transistor by incorporating Al into host La ₂ O ₃ as gate dielectric. Nanotechnology, 2021, 32, 305201.	2.6	5
85	Low-Power OR Logic Ferroelectric In-Situ Transistor Based on a CulnP2S6/MoS2 Van Der Waals Heterojunction. Nanomaterials, 2021, 11, 1971.	4.1	5
86	Preparation and Research of Monolayer WS2 FETs Encapsulated by h-BN Material. Micromachines, 2021, 12, 1006.	2.9	5
87	Research on Total Ionizing Dose Effect and Reinforcement of SOI-TFET. Micromachines, 2021, 12, 1232.	2.9	5
88	Polarization Gradient Effect of Negative Capacitance LTFET. Micromachines, 2022, 13, 344.	2.9	5
89	Polarization properties in grating-gated AlN/GaN HEMTs at mid-infrared frequencies. Optics Express, 2022, 30, 14748.	3.4	5
90	Hybrid Nanowire–Rectangular Plasmonic Waveguide for Subwavelength Confinement at 1550 Nm. Micromachines, 2022, 13, 1009.	2.9	5

#	Article	IF	CITATIONS
91	Electrical properties and interfacial issues of high- <i>k</i> /Si MIS capacitors characterized by the thickness of Al2O3 interlayer. AlP Advances, 2016, 6, .	1.3	4
92	Effects of Rapid Thermal Annealing and Different Oxidants on the Properties of LaxAlyO Nanolaminate Films Deposited by Atomic Layer Deposition. Nanoscale Research Letters, 2017, 12, 218.	5.7	4
93	Analog/RF performance of two tunnel FETs with symmetric structures. Superlattices and Microstructures, 2017, 111, 568-573.	3.1	4
94	The Optimization of Spacer Engineering for Capacitor-Less DRAM Based on the Dual-Gate Tunneling Transistor. Nanoscale Research Letters, 2018, 13, 73.	5.7	4
95	Impact of remote oxygen scavenging on the interfacial characteristics of atomic layer deposited LaAlO3. Materials Science in Semiconductor Processing, 2019, 90, 50-53.	4.0	4
96	Comprehensive Performance Quasi-Non-Volatile Memory Compatible with Large-Scale Preparation by Chemical Vapor Deposition. Nanomaterials, 2020, 10, 1471.	4.1	4
97	TCAD Simulation of the Doping-Less TFET with Ge/SiGe/Si Hetero-Junction and Hetero-Gate Dielectric for the Enhancement of Device Performance. Coatings, 2020, 10, 278.	2.6	4
98	Low-power design and application based on CSD optimization for a fixed coefficient multiplier. Science China Information Sciences, 2011, 54, 2443-2453.	4.3	3
99	Molecular dynamics simulation of latent track formation in bilayer graphene. IEICE Electronics Express, 2015, 12, 20150771-20150771.	0.8	3
100	Research on the origin of negative effect in uniform doping GaN-based Gunn diode under THz frequency. Applied Physics A: Materials Science and Processing, 2016, 122, 1.	2.3	3
101	The Effect of Ion Irradiation Density on the Defect of Graphene: A Molecular Dynamics Study. Crystals, 2020, 10, 158.	2.2	3
102	Adjusting transmissivity based on grapheme–h-BN–graphene heterostructure as a tunable phonon–plasmon coupling system in mid-infrared band. Journal of Materials Science, 2021, 56, 3210-3219.	3.7	3
103	A subwavelength high modulation depth optical modulator based on bilayer graphene. Optical Materials, 2021, 117, 111139.	3.6	3
104	A waveguide-integrated graphene-based subwavelength electro-optic switch at 1550 nm. Optics Communications, 2021, 495, 127121.	2.1	3
105	Interface optimization of La-based gate dielectric for molybdenum disulfide field-effect transistors. Applied Surface Science, 2022, 581, 152248.	6.1	3
106	The Image Identification Application with HfO2-Based Replaceable 1T1R Neural Networks. Nanomaterials, 2022, 12, 1075.	4.1	3
107	Electrical and Thermal Characteristics of AlGaN/GaN HEMT Devices with Dual Metal Gate Structure: A Theoretical Investigation. Materials, 2022, 15, 3818.	2.9	3
108	Interaction of NBTI with Hot Carriers in PMOSFET's for Advanced CMOS Technologies. , 2006, , .		2

#	Article	IF	CITATIONS
109	An analytical model of anisotropic low-field electron mobility in wurtzite indium nitride. Applied Physics A: Materials Science and Processing, 2014, 114, 1113-1117.	2.3	2
110	Effects of total dose irradiation on the threshold voltage of H-gate SOI NMOS devices. Nuclear Science and Techniques/Hewuli, 2016, 27, 1.	3.4	2
111	Multiscale simulations of swift heavy ion irradiation effect on bilayer graphene. IEICE Electronics Express, 2016, 13, 20151040-20151040.	0.8	2
112	Band alignments of La x Al y O films on Si substrates grown by atomic layer deposition with different La/Al atomic ratios. Journal of Materials Science: Materials in Electronics, 2017, 28, 4702-4705.	2.2	2
113	Improvement of the high- \hat{l}^{e} /Ge interface thermal stability using an in-situ ozone treatment characterized by conductive atomic force microscopy. Chinese Physics B, 2017, 26, 087701.	1.4	2
114	The influence of La/Al atomic ratio on the dielectric constant and band-gap of stack-gate La–Al–O/SiO2 structure. Journal of Materials Science: Materials in Electronics, 2017, 28, 2004-2008.	2.2	2
115	The Influence of Copper Substrates on Irradiation Effects of Graphene: A Molecular Dynamics Study. Materials, 2019, 12, 319.	2.9	2
116	Synthesis and Spectral Characteristics Investigation of the 2D-2D vdWs Heterostructure Materials. International Journal of Molecular Sciences, 2021, 22, 1246.	4.1	2
117	Construction and electrical performance improvement of MoS ₂ FET with graphene/metal contact. Optical Materials Express, 2021, 11, 3099.	3.0	2
118	Atomic Layer Deposition of Ultrathin La2O3/Al2O3 Nanolaminates on MoS2 with Ultraviolet Ozone Treatment. Materials, 2022, 15, 1794.	2.9	2
119	A new method of thin gate SiO2 reliability characterization. Surface and Interface Analysis, 2002, 34, 437-440.	1.8	1
120	Anisotropic longitudinal electron diffusion coefficient in wurtzite gallium nitride. Applied Physics A: Materials Science and Processing, 2013, 112, 933-938.	2.3	1
121	Anisotropic lowâ€field electron diffusion coefficient and mobility in wurtzite indium nitride. Physica Status Solidi (B): Basic Research, 2014, 251, 168-171.	1.5	1
122	Total ionizing dose effect of gamma rays on H-gate PDSOI MOS devices at different dose rates. Nuclear Science and Techniques/Hewuli, 2017, 28, 1.	3.4	1
123	Impacts of the Oxygen Precursor on the Interfacial Properties of LaxAlyO Films Grown by Atomic Layer Deposition on Ge. Materials, 2017, 10, 856.	2.9	1
124	Research of Heterogeneous Acceleration Optimization of Convolutional Neural Network Algorithm for Unmanned Vehicle Based on FPGA. , 2019, , .		1
125	Filtering Characteristics of Phonon Polaritons Waves Based on Dielectric-h-BN-Dielectric Structure in Mid-Infrared Band. Nanomaterials, 2020, 10, 878.	4.1	1
126	Robust and Latch-Up-Immune LVTSCR Device with an Embedded PMOSFET for ESD Protection in a 28-nm CMOS Process. Nanoscale Research Letters, 2020, 15, 212.	5.7	1

#	Article	IF	CITATIONS
127	DC and pulsed DC stress evolution in copper interconnects. , 2006, , .		0
128	Numerical Analysis of Barrier Layer Effect on Copper Electromigration. , 2006, , .		0
129	Characteristics analysis and optimization design of a new ESD power clamp circuit. Microelectronics Reliability, 2010, 50, 1087-1093.	1.7	Ο
130	Investigation of electrical characteristics of NdAlO <inf>3</inf> /SiO <inf>2</inf> stack gate. , 2010, , .		0
131	Modeling of enhancement factor of hole mobility for strained silicon under low stress intensity. Microelectronics Reliability, 2011, 51, 909-913.	1.7	0
132	A modified ESD clamp circuit for 90-nm CMOS process. , 2012, , .		0
133	Off-state leakage current of nano-scaled MOSFETs with high-k gate dielectric. , 2012, , .		0
134	A novel ESD power supply clamp circuit with double pull-down paths. Science China Information Sciences, 2013, 56, 1-8.	4.3	0
135	Enhanced Electrical Properties of Atomic Layer Deposited LaxAlyO Thin Films with Stress Relieved Preoxide Pretreatment. Materials, 2018, 11, 1601.	2.9	0
136	Impact of Al+ implantation on the Switching Characteristics of Al2O3/La2O3/Al2O3 multilayer RRAM devices. , 2019, , .		0
137	Enhanced Interfacial Characteristics of Atomic Layer Deposited LaAlO3 Thin Films. , 2019, , .		0
138	Simulation of Displacement Damage in Nanoscale MOSFET Caused by Galactic Cosmic Rays. Journal of Computational and Theoretical Nanoscience, 2016, 13, 5242-5246.	0.4	0
139	Research on Transparent Resistive Random Memory Based on Lanthanum-based High-k Medium. , 2021, , .		0
140	Investigation of Negative Bias Temperature Instability Effect in Nano PDSOI PMOSFET. Micromachines, 2022, 13, 808.	2.9	0